HHS Public Access

Author manuscript

Bone. Author manuscript; available in PMC 2021 June 30.

Published in final edited form as:

Bone. 2019 November ; 128: 115031. doi:10.1016/j.bone.2019.08.004.

Osteocalcin Affects Bone Mineral and Mechanical Properties in Female Mice.

O. Berezovska[1], **G. Yildirim**[1], **W. Budell**[2], **S. Yagerman**[3], **B. Pidhaynyy**[2], **C. Bastien**[1], **M.C.H. van der Meulen**[3,4], **T.L. Dowd**[*,1,5]

[1]Department of Chemistry, Brooklyn College, Brooklyn, N.Y. 11210,

[2]Department of Biology, Brooklyn College, Brooklyn, N.Y. 11210

[3]Meinig School of Biomedical Engineering and Sibley School of Mechanical & Aerospace Engineering, Cornell University, Ithaca N.Y.

[4]Research Division, Hospital for Special Surgery, NY, NY

[5]Ph.D. Program in Chemistry and Ph.D. Program in Biochemistry, The Graduate Center of the City University of New York, New York, NY 10016

1.0 INTRODUCTION

Osteocalcin is a small (49 aa, 5850 MW) protein synthesized by osteoblasts and osteocytes and one of the most abundant noncollagenous proteins in bone [1, 2]. Osteocalcin production is stimulated by vitamin D [3]. The protein contains 3 gamma-carboxy glutamic acid (3 Gla-Ost) residues made post-translationally in a vitamin K-dependent process [4]. The 3 γ- carboxyglutamic acid residues can bind Ca^{2+} or divalent cations in solution and in hydroxyapatite mineral. Calcium can induce a conformational change that increases the binding of osteocalcin to mineral hydroxyapatite [5–7]. *In-vivo*, the 3-Gla osteocalcin is mainly bound to bone mineral, with lower concentrations in the serum [8, 9]. Earlier studies demonstrated osteocalcin affected bone mineral formation and mineral crystal growth in solution [10, 11]. It was also involved in the recruitment, differentiation and maturation of osteoclasts [12–14]. A previous report using female osteocalcin-depleted knock-out mice on a mixed genetic background (129/B6) demonstrated that osteocalcin inhibited bone formation, had no effect on bone resorption, and decreased cortical thickness resulting in bones of reduced strength in the wild-type mice [15]. A later study using similar mice found that osteocalcin affected crystal size, mineral maturity and bone remodeling [16]. More recently in 6-month-old male osteocalcin knock-out mice on a C57BL/6J (B6) pure background, osteocalcin regulated mineral crystal size and organization [17], and reduced

[*]Address for Correspondence: Terry L. Dowd, Department of Chemistry Rm. 359 NE, Brooklyn College of the City University of New York, 2900 Bedford Ave., Brooklyn, New York 11210. Ph: 718-951-5000 ×2847 Fax: 718-951-4607, TDowd@brooklyn.cuny.edu.

Declaration of Interest

All authors declare they have no conflict of interest.

maximum bending load but did not alter stiffness or ultimate strength [18]. In wild-type male mice on a B6 pure background, osteocalcin improved bone material properties with enhanced fracture resistance through the formation of dilational bands composed of osteocalcin and osteopontin [19, 20].

The variable effects on bone strength parameters suggest that the genetic background (mixed 129/B6 vs pure B6) and sex may play a role in the phenotype of osteocalcin knock-out mice. Analyzing a mutation on different genetic backgrounds and between sexes is critical to our understanding of the protein's role. The B6 is a well-defined background, yet adult female osteocalcin knockout mice have not been examined on a pure B6 background [19]. Bone strength is a function of geometry, bone mineral content, tissue material properties and bone turnover. Osteocalcin plays a role in bone material quality, bone turnover and perhaps also fracture resistance. Reduced bone strength and fractures in the elderly are very common, and osteocalcin decreases with age [8, 21, 22] and in some diseases [8, 23]. Therefore, the effect of osteocalcin on bone strength and material properties in female adult mice is of interest.

This study compared bone mineral and mechanical properties in the presence and absence of osteocalcin between adult female age- and B6 background-matched wild-type and osteocalcin knock-out mice. Bone turnover was assessed by biomarkers for bone formation (P1NP) and resorption (CTX) measured in serum. The number of osteoclasts and osteoblasts per bone perimeter were measured by histomorphometry. Fourier Transform Infrared Imaging (FTIRI) was used to measure detailed mineral properties such as mineral/matrix ratio, bone crystal size and perfection, collagen maturity, carbonate/mineral ratio and acid phosphate content in mineral. Bone mineral density and geometry were investigated using quantitative microcomputed tomography (microCT) and whole bone strength was measured in three-point bending.

2.0 MATERIALS AND METHODS

2.1 Experimental Animals

Osteocalcin deficient mice were provided by Gerard Karsenty, on a mixed 129/B6 background, as described [15]. Congenic strains were generated in the lab of Dr. Caren Gundberg by back-crossing to a C57BL/6J (B6) background for 10 generations using animals purchased from Jackson Laboratories (Bar Harbor, Maine). Genotypes were identified by PCR using DNA extracted from a 3-mm tail specimen using specific oligonucleotide primers for osteocalcin and the neo insert. The serum samples and femora from 6 month old female wild-type and osteocalcin knockout mice were obtained from Dr. Caren Gundberg and used for this experiment. All animal protocols were approved by the IACUC of the institute providing the bones (Yale Medical School) and the IACUC committee of Brooklyn College.

Blood samples were collected via periorbital blood collection before sacrifice. Serum was obtained from these blood samples for bone biomarker measurements. At euthanasia, the right and left femora and tibia from each animal were dissected and cleaned of soft tissue. One femur was used for FTIRM, and the second femur was used for microcomputed tomography (microCT) and whole bone mechanical measurements. Bone calcium and

calcium/phosphate ratios were measured on the marrow-depleted tibial diaphysis using Atomic Absorption for calcium and a colorimetric method for phosphate [24].

2.2 Bone Biomarker Measurements

The bone formation marker P1NP and the bone resorption marker CTX were assayed in serum collected at euthanasia from wild-type and osteocalcin knock-out mice. Serum P1NP and CTX (RatLaps) were assayed by rodent specific kits (Immunodiagnostic Systems Inc, Fountain Hills, AZ) [25, 26].

2.3 Histomorphometry

Mouse femora were processed and embedded in polymethyl methacrylate. Five micron thick calcified sections were placed on silane-coated slides, deplasticized and stained with toluidine blue. Static Histomorphometry was performed on the endocortical surface of bones from wild-type and osteocalcin knock-out mice at a magnification of x10. The following measurements were obtained: cortical tissue area, cortical bone area, eroded perimeter, marrow area, bone perimeter, mineralized perimeter, number of osteoblasts and number of osteoclasts. The measurements were obtained using Osteomeasure software (Osteometrics, Atlanta, GA., U.S.A.).

2.3 Microcomputed Tomography (microCT)

MicroCT was used to provide information on 3-D cortical bone structure. Femora were scanned in PBS with a 15 μm voxel size, 55 kVp, 0.36 degrees rotation step (360 degrees angular range) and a 400 ms per view exposure (Scanco μ-CT 35 system, Scanco Medical, Basserdorf, Switzerland). A 0.47 mm segment of the mid-diaphysis was analyzed with thresholding at 0.4g/cc. Three-dimensional reconstruction and image viewing were performed with Scanco system software (HP, DECwindows Motif 1.6).

Cortical bone parameters included bone tissue mineral density (TMD) which is calculated from the average attenuation of bone tissue exclusively and does not include attenuation from non-bone voxels. The attenuation coefficient measured by microCT is converted to physical density in units of mg HA/cm^3. Other cortical parameters include total and bone volumes, bone-volume-to-total volume ratio (BV/TV), cortical thickness, the polar moment of inertia (J) and minimum and maximum area moment of inertia (I_{min}, I_{max}). The moment of inertia, *I*, is a geometric measure of the resistance of an area to bending. *I* is based on the tissue distribution in the cross section and does not account for material properties. Any given cross section has an orientation of minimum and maximum *I* that are about perpendicular planes.

Trabecular bone parameters included total and bone volumes, bone volume/total volume, connectivity density, trabecular number, trabecular thickness, trabecular spacing and tissue mineral density.

2.4 Whole bone mechanical testing

The whole bone bending stiffness and strength were measured by loading the femora to failure in three-point bending in a servohydraulic testing system (MiniBionix 858, MTS

Systems,Eden Prairie, MN and MLP 25 load cell, Transducer Techniques, Temecullah CA). Each femur was positioned with the posterior surface on the supports (7.1mm span). This loading orientation corresponded to bending about the plane of the minimum moment of inertia (I_{min}). The load was applied to the anterior surface at a constant rate of 0.1mm/sec, and load and displacement data were sampled at 20 Hz.

The load-displacement curves were analyzed for whole bone properties including bending stiffness and maximum bending moment. The bending stiffness (EI, N*mm2) is the resistance of the whole bone to deformation for a given load. Bending stiffness captures both material and geometric contributions to the whole bone bending behavior. The maximum bending moment is the highest bending load sustained before failure of the whole bone and is commonly referred to as the strength of the whole bone. Adjusting the bending stiffness and maximum bending moment for cross-sectional geometric contributions to strength with I_{min} allows the relative contributions of material properties and bone size to be understood. In this context, material properties refers to all possible tissue contributions that are not reflected by the cortical geometry. The material properties are influenced by bone composition such as mineral density, mineral stoichiometry, collagen content, crosslink maturity, bone crystal size and bone turnover [27].

2.5 Fourier-transform infrared imaging (FTIRI).

To measure mineral and matrix composition by spectroscopy, femora were cleaned of soft tissue, processed and embedded in polymethylmethacrylate (PMMA) according to standard protocol [28]. Spectral images were collected at a 4 cm^{-1} spectral resolution and ~7 μm spatial resolution from 2 μm thick longitudinal sections mounted on infrared windows (Spotlight 400 Imaging system, Perkin Elmer Instruments, Shelton, CT USA). Background spectra were collected under identical conditions from clear Ba_2F windows and subtracted from sample data by instrumental software. IR spectra were collected from three areas (~ 500 μm × 500 μm) of cortical bone per sample. After acquisition, all spectra were baseline-corrected, normalized to the PMMA peak at 1728 $cm^{-1}$and the spectral contribution of PMMA embedding media was subtracted using ISYS Chemical Imaging Software (Malvern, Worcestershire, UK). Spectroscopic parameters of mineral-to-matrix ratio, crystallinity, carbonate-to-mineral ratio, collagen maturity and acid phosphate were calculated [29]. The mineral-to-(collagen)-matrix ratio was the integrated area ratio of the v_1 v_3 PO_4 band (900–1200 cm^{-1}) / amide I band (1590–1712 cm^{-1}), the mineral crystallinity parameter corresponds to the crystallite size and perfection as determined by x-ray diffraction and is calculated from the intensity ratios of subbands at 1030 cm^{-1} (stoichiometric apatite) and 1020 cm^{-1} (nonstoichiometric apatite) [30]. The carbonate to mineral ratio is the integrated area ratio of the carbonate peak (850–890)/ v_1 $_{v3}$ PO_4 band (900–1200 cm^{-1}) . The collagen maturity parameter is the ratio of nonreducible (mature) to reducible (immature) collagen cross-links, which is expressed as the intensity ratio of 1660 cm^{-1} /1690 cm^{-1} [31] . The acid phosphate content in the mineral is measured from the peak height ratio of 1128/1096 [32]. The results for each parameter were expressed as a histogram describing the pixel distribution giving the mean value of the distribution and associated color coded images were generated at the same time by ISYS.

2.6 Statistical Methods

Data for each measured parameter are expressed as mean ± standard error of the mean for each group The data for nearly all measured parameters were found to be normally distributed as analyzed by the Shapiro-Wilk test. Data from those parameters were compared by the Student's independent t-test for significant differences between groups. Parameters whose data was not normally distributed were compared using the Mann-Whitney rank test. Differences for each measured parameter were considered statistically significant when $p \leq 0.05$. A trend is defined as a p-value within the range $0.10 \geq p \geq 0.05$. All reported results are significant unless stated.

3.0 RESULTS

3.1 Bone Ca^{2+} measurements.

Bone calcium concentration, as measured by atomic absorption, was not different between the osteocalcin knock-out (OC−/−) and wild-type (OC+/+) mineral (354 ± 8 and 338 ± 4 mg Ca/g ash, respectively). Ca/P molar ratio was not different between the OC+/+ and OC−/− (1.493 ± 0.07 and 1.516 +/− 0.02, respectively).

3.2 Microcomputed Tomography and Biomechanical Measurements

MicroCT scans were collected on femora from OC+/+ and OC−/− mice. The femoral diaphysis of the OC+/+ cortex had a small but significantly higher bone mineral density as compared to OC−/−. No significant difference was found for the other morphological parameters between the OC+/+ and OC−/− cortical bones (Table IA).

MicroCT data for the trabecular bone is given in Table IB. A significant increase in the bone volume, bone volume/total volume, connectivity density and trabecular number were seen in the OC−/− vs. OC+/+ bones. A significant reduction in trabecular spacing was observed in the OC−/− as compared to OC+/+ trabecular bone.

Mechanical properties were measured in the two groups (Table II). Bending stiffness (EI) was significantly decreased in the OC−/− bones as compared to the OC+/+ bones. Similarly, the maximum bending moment was lower in the OC−/− bones versus the OC+/+. To determine whether differences in stiffness or maximum bending moment were due to bone geometry or tissue material properties, the parameters were normalized by the moment of inertia corresponding to the plane of bending testing (I_{min}), a measure of the geometric resistance to bending. If normalization by Imin removes the differences in these parameters (between OC−/− and Oc+/+ bones) then the effect was due to a difference in size or geometry of the bones. The OC−/− bones had a trend toward a significantly lower size-adjusted bending stiffness (EI/I_{min}) compared to the OC+/+ femora ($p = 0.056$). Based on these normalized results, the decreased bending stiffness in the OC−/− cortical tissue resulted from differences in material properties in the knock-out mice, not differences in cortical geometry. To understand the effect of bone size, the maximum bending moment (M_{max}) was also normalized by I_{min}. The OC−/− had a significantly reduced (11%) M_{max}/I_{min} compared to OC+/+, indicating the difference in the maximum bending moment in the OC−/− bones compared to the OC+/+ bones was due to decreased material properties.

3.3 Fourier Transform Infrared Imaging

Fourier Transform Infrared Imaging (FTIRI) composition data were collected on the cortices of the OC−/− and OC+/+ groups. Representative color-coded images are shown in Figure 1 with plotted values in Figure 2. The images showed that the OC−/− bones had a reduced ($p<0.001$, n=9) mineral-to-matrix ratio as compared to the OC+/+ bone tissue. The crystallinity parameter, related to bone crystal size and hydroxyapatite perfection, was significantly reduced as well ($p<0.005$) in the OC−/− mineral as compared to the OC+/+. Hydroxyapatite perfection/maturity refers to how close the mineral is to hydroxyapatite stoichiometry (Ca_{10} $(PO_4)_6$ $(OH)_2$). Acid phosphate (HPO_4^{2-}) ion can substitute into the apatite bone matrix and is increased in young, immature bone and decreases in older bone [32]. An increased acid phosphate content ($p<0.01$) was observed in OC−/− mineral as compared to OC+/+, indicating an increase in new bone formation. The increased HPO_4^{2-} content can be observed along the outer surfaces of the bone where new mineral deposition occurs, while the older mineral is in the center of the cortex showing low amounts of HPO_4^{2-} (Figure 1). The CO_3^{2-} ion can also substitute into the apatite bone matrix and replace PO_4^{3-} or OH^-. The OC−/− mineral had a significantly increased carbonate to phosphate ratio as compared to the OC+/+ mineral ($p < 0.05$). This indicates more CO_3^{2-} in the OC−/− mineral. No difference was observed between the groups in the collagen maturity, which is the ratio of the mature nonreducible crosslinks to the immature reducible crosslinks.

3.4 Serum Biomarkers and Matrix Osteocalcin

Bone formation and resorption were measured using serum biomarkers P1NP and CTX respectively. In addition to these bone turnover markers the number of osteoblasts and osteoclasts were determined per bone perimeter (Table III) by histomorphometry. The serum P1NP concentration was increased in the absence of osteocalcin ($p<0.05$) as compared to the OC+/+ bones (Figure 3), indicating increased bone formation in the OC−/− bones. Table III shows the histomorphometry results indicate a significant increase in the number of osteoblasts/bone perimeter in the OC−/− vs. OC+/+. On the other hand, bone resorption, as indicated by serum CTX concentration, was not different between OC+/+ and OC −/− mice. The number of osteoclasts/bone perimeter was not significantly different between the OC−/− and OC+/+ mice as well. In addition, we observe no difference in marrow area nor marrow area/total area between the OC−/− and OC+/+ bones also suggesting no difference in bone resorption (Table I). The results indicate an imbalance in bone turnover in the OC−/− with greater formation than resorption.

4.0 DISCUSSION

This study is the first to investigate the role of osteocalcin in both mineral and mechanical properties in female mice on a pure B6 genetic background. Bone mineral and matrix properties were compared in the presence and absence of osteocalcin. The bone remodeling parameters and histomorphometric data help explain the results obtained when comparing the two groups of mice.

We found the bone mineral density and mineral-to-matrix ratio were significantly reduced in the OC−/− vs. OC+/+ mice. The average cortical bone volume in the OC−/− was higher,

though not significantly, and that could contribute to a slightly lower (2%) bone mineral density. Also the increased amount of carbonate (CO_3^{2-}) in the OC−/− mineral could contribute as well. The (CO_3^{2-}) ion can replace PO_4^{3-} in the apatite crystal lattice. The microCt image is a map of attenuation coefficients. The attenuation coefficient depends on the atomic number of the elements present, their weight fractions and the density of the material. The higher the attenuation factor the higher the tissue density. Since C has a lower atomic number than P, the increased substitution of CO_3^{2-} for PO_4^{3-} in the mineral would alter the attenuation factor leading to a slight decrease in bone mineral density. The reduction in mineral to matrix ratio in the OC−/− cortical bones can be explained by the imbalance in the bone turnover seen in OC−/−. The knockout mouse on a mixed 129/ B6 background had a higher bone formation rate with no change in resorption [15]. This finding was explained by the osteoblasts in the OC −/− mice producing more bone matrix than the wild-type mice [15]. Our bone biomarkers corroborate this prior result and reveal an increase in bone formation (P1NP) with no change in bone resorption (CTX) in the Ost −/− versus the OC +/+ control. In addition we find a significant increase in the number of osteoblasts /bone perimeter in the OC−/− bones, no difference in the number of osteoclasts/ bone perimeter and no difference in bone marrow area (related to bone resorption) between the OC−/− and OC+/+ bones. Altogether these results strongly suggest an imbalance in bone turnover with increased bone formation and no change in resorption in the OC−/− bones. This imbalance in turnover would produce an increased amount of collagen matrix being deposited by the osteoblasts in OC −/− mice and not resorbed. The amount of mineral (calcium) was not significantly different between OC−/− and OC+/+, and is not responsible for the decrease in mineral/matrix ratio. The increased matrix was retained in the OC−/− because bone resorption, which would remove the matrix during remodeling, did not scale with the increased formation.

We find significantly higher trabecular bone volume/total volume, connectivity density, and trabecular number in the OC−/− vs. OC+/+ mice which is in agreement with a previous study reporting increased trabecular bone in the osteocalcin knock-out on a mixed background [15]. The increased trabecular bone also supports an increased bone formation without an increase in bone resorption in the OC−/−.

The OC−/− bones had significantly reduced crystallinity as compared to the OC+/+ tissue. This result is in agreement with a previous FTIR imaging study in female OC−/− mice that reported decreased crystallinity and immature mineral phase in the knockout mouse from a mixed 129/B6 background [16]. The crystallinity parameter (1030/1020 peak height ratio) reflects the size and stoichiometric perfection of the hydroxyapatite crystals ($Ca_{10}(PO_4)_6(OH)_2$). Although the Ca/P ratios were not significantly different between the knock-out and wild-type bones, the increase in HPO_4^{2-} and CO_3^{2-} substitution in the OC−/− mineral could contribute to a reduction in the crystallinity parameter by decreasing the stoichiometric perfection of the lattice. In addition, there may also be a decrease in mineral crystal size in the knock-out mice which contributes to a decrease in this parameter. The smaller crystal size was previously reported with warfarin treatment [33, 34] and was interpreted as osteocalcin inhibiting or delaying nucleation. More recently data from male OC−/− mice on a pure B6 background suggested that the small crystal size in the knock-out bone could be due to poorly regulated mineral apposition resulting in loose mineral

aggregates [17]. The increased bone formation can also explain, in part, why the bone crystal size would be significantly reduced in the OC−/− bone tissue. Smaller crystals reflect newly formed bone that has not yet been remodeled. Increased bone formation rates are associated with a smaller crystal distribution, which may have been deposited quickly. These early mineral deposits in bone contain elevated concentrations of HPO_4^{2-} ions that are present in young, immature bone [32, 35]. More early mineral deposits containing HPO_4^{2-} ions would be expected in bones with a higher bone formation rate (OC−/−) as compared to those with a lower bone formation rate (OC+/+). This results in an immature mineral phase because the increase in bone formation is not balanced by an increase in bone resorption in the OC−/− animals. A previous FTIR imaging study on OC−/− mice on a mixed background also found a more immature mineral phase in the OC−/− vs. OC+/+ mineral [16].

The significant decrease in the mineral-to-matrix ratio in the OC−/− bones, due to the imbalance in bone turnover, helps explain the observed decrease in cortical bending stiffness (EI) and the trend toward a decreased size-adjusted bending stiffness (EI/I_{min}) in the OC−/− bones as opposed to that of OC+/+ femora. The cortical matrix which is retained in the OC −/− mice would lead to more compliant bones. The trend toward a reduction in the EI/I_{min} values in the OC−/− bones suggests that reduced stiffness is not due to geometry or size but rather to decreased material quality. We also observed a significant decrease in the maximum bending load (M_{max}) and the size-adjusted M_{max}/I_{min} values in the OC−/− as compared to the OC+/+ bones. The parameter M_{max} is the maximum load or force withstood before fracturing. As for stiffness, the decrease in M_{max}/I_{min} indicates the reduction in strength is not due to geometry or size but poor material quality. Tissue material properties are influenced by ‘bone quality’ factors such as organization of mineral and crystallite size and perfection, collagen crosslinks, microarchitecture and presence of microcracks [36, 37]. The significant reduction in bone mineral density, mineral-to-matrix ratio and crystallinity [38] seen in the OC−/− bones can help explain the reduction in bone strength and material quality.

Several studies in males on a B6 background measured whole bone strength or material properties in the OC−/− at 6 months of age. One study found the male OC−/− displayed a significantly higher maximum bending moment, and no difference in stiffness or size-adjusted ultimate strength as compared to the OC+/+ [18]. In our results M_{max} was lower for the female OC−/− as compared to the OC+/+ bones, and this difference was not due to size or geometry of the bone. This discrepancy could be due to differences in male and female mice. Similar to humans [39], wild-type male mice were reported to have greater periosteal bone formation and expansion resulting in stronger bones as compared to female wild-type mice [40]. This trend could be seen in male OC−/− vs. female OC−/− as well. The knockout has increased bone formation that would further increase the periosteal expansion as compared to the male wild-type mouse cortical bone. Indeed the values for total area and I_{min} are larger for the male OC−/− than OC+/+ bone although not significantly [18] . When the M_{max} values were adjusted for size, this lack of effect would explain the lack of difference in ultimate strength between the two groups.

Other studies in the male B6 mice revealed the direct structural roles of osteocalcin and osteopontin in energy dissipation in bone through the formation of dilatation bands between

mineralized collagen fibrils when microdamage was present in bone. Male osteocalcin knockout mice on the same B6 background had no osteocalcin and consequently no dilatational bands. This would significantly lower amounts of diffuse damage, signifying an increased propensity to fracture [19, 20]. The lack of dilational bands in OC−/− bone tissue could contribute to weaker bone and material properties in the knock-out, further corroborating our findings on this background.

In conclusion, the animal genetic background and sex can influence the phenotype of a mutant strain. Therefore, mutations need to be examined on different backgrounds. Some reported properties of the OC−/− skeleton appear to be dependent on the genetic background of the mice while others are independent of background. The female KO mice on the B6 background in this study had a significantly increased bone formation rate, decreased crystallinity, an immature mineral phase and no change in bone resorption as compared to the OC+/+ mice. This result is in agreement with the previous studies of the female OC−/− on a mixed 129/B6 background [15, 16]. However, the increased cortical thickness, increased bone mineral density and increased strength reported in the 129/B6 OC−/− vs. the OC+/+ bones [15] were not observed in the B6 OC−/− vs. the OC+/+ bones. Instead a decreased bone mineral density, decreased mineral/matrix ratio, decreased whole bone stiffness and decreased whole bone strength due to reduced material quality were observed in the OC−/− vs. OC+/+ bones on the pure B6 background. These differences are most likely due to the different genetic backgrounds in the mice. A previous study found particular combinations of morphological and compositional traits separate femurs according to genetic background [41]. These trait distributions predicted whole bone biomechanical differences between the strains. The 129 strain had significantly higher cortical area and moment of inertia and this correlated with a higher stiffness and maximum load in the 129 as compared to B6 groups. Mice from a 129/B6 mixed background are not genetically uniform and would contain a variable mixture of both backgrounds. A portion of the phenotype from the OC−/− may not be exactly the same on this background as compared to a genetically pure B6 background.

The results in this study show that female osteocalcin knock-out mice have weaker bone material properties and diminished bone strength on a specific genetic background. Osteocalcin decreases with age [8, 21, 22] and with some diseases such as diabetes [8, 23]. Bone tissue becomes weaker and more prone to fracture with age [42, 43]. Bone abnormalities and fracture risk are also higher in diabetes and underpredicted by bone mineral density, strongly suggesting an impairment of bone material properties [44, 45]. Given the genetic heterogeneity in the human population, our results suggest that reduced osteocalcin levels could be a contributing factor to weaker bone strength and fracture risk in certain groups of the elderly or diabetic patients.

Acknowledgements

The authors would like to thank Dr. Gerard Karsenty and Baylor College for allowing the use of the osteocalcin knock-out tissue. We would also like to thank Dr. Caren Gundberg for backcrossing the osteocalcin knock-out mice onto a C57BL/6J background and providing the bone and serum samples for our study. The authors are also thankful to the late Dr. Adele Boskey, Dr. Patricia Ducy, Dr. Stephen Doty and Dr. Deepak Vashishth for informative discussions and to Lyudmila Spevak and Lyudmila Lukashova for technical advice. Support for some of this project was provided by NIH grant ES-009032 to T.D.

Abreviations:

Gla	γ – carboxyglutamic acid
B6	C57BL/6J mice
OC+/+	wild-type
OC−/−	osteocalcin knock-out
FTIRI	Fourier Transform Infrared Imaging

REFERENCES

[1]. Hauschka PV, Lian JB and Gallop PM , Direct identification of the calcium binding amino acid, γ-carboxyglutamate in mineralized tissue. , Proc. Natl. Acad. Sci. USA 72 (1975) 3925–3929 [PubMed: 1060074]

[2]. Price PA, Otsuka AS, Poser JW, Kristaponis J and Raman N, Characterization of a γ-carboxyglutamic acid containing protein from bone., Proc. Natl. Acad. Sci. USA 73 (1976) 1447–1451 [PubMed: 1064018]

[3]. Lian JB, Glimcher MJ, Roufosse AH, Hauschka PV, Gallop PM, Cohen-Solal L, Reit B, Alterations of the gamma-carboxyglutamic acid and osteocalcin concentrations in vitamin D-deficient chick bone, J. Biol. Chem 257(9) (1982) 4999–5003. [PubMed: 6802844]

[4]. Berkner KL, The vitamin K-dependent carboxylase, Annu Rev Nutr 25 (2005) 127–49. [PubMed: 16011462]

[5]. Dowd T, Rosen J, Li L, Gundberg C, The three-dimensional structure of bovine calcium ion-bound osteocalcin using 1H NMR spectroscopy, Biochemistry 42(25) (2003) 7769–7779. [PubMed: 12820886]

[6]. Hoang QQ, Sicheri F, Howard AJ, Yang DS, Bone recognition mechanism of porcine osteocalcin from crystal structure, Nature 425(6961) (2003) 977–80. [PubMed: 14586470]

[7]. Dowd T, Rosen J, Mints L, Gundberg C, The effect of Pb^{2+} on the structure and hydroxyapatite binding properties of osteocalcin, Biochim. Biophys. Acta (BBA)-Molecular Basis of Disease 1535(2) (2001) 153–163. [PubMed: 11342004]

[8]. Hauschka PV, Lian JB, Cole DEC and Gundberg CM, Osteocalcin and Matrix Gla proteins: Vitamin K-Dependent Proteins in Bone, Physiol. Rev 69 (1989) 990–1047. [PubMed: 2664828]

[9]. McKee MD, Farach-Carson MC, Butler WT, Hauschka PV and Nanci A, Ultrastructural immunolocalization of noncollagenous, (osteopontin and osteocalcin) and plasma (albumin and α2 HS-glycoprotein) proteins in rat bone, J. Bone Min. Res 8 (1993) 485–496.

[10]. Hunter GK, Hauschka PV, Poole AR, Rosenberg LC, Goldberg HA, Nucleation and inhibition of hydroxyapatite formation by mineralized tissue proteins, Biochem. J 317(Pt 1) (1996) 59. [PubMed: 8694787]

[11]. Romberg RW, Werness PG, Riggs BL, Mann KG, Inhibition of hydroxyapatite-crystal growth by bone-specific and other calcium-binding proteins, Biochemistry 25(5) (1986) 1176–1180. [PubMed: 3008822]

[12]. Lian J, Tassinari M, Glowacki J, Resorption of implanted bone prepared from normal and warfarin-treated rats, J. Clin. Invest 73(4) (1984) 1223. [PubMed: 6608532]

[13]. Liggett WH, Lian JB, Greenberger JS, Glowacki J, Osteocalcin promotes differentiation of osteoclast progenitors from murine long-term bone marrow cultures, J. Cell. Biochem 55(2) (2004) 190–199.

[14]. Ishida M, Amano S, Osteocalcin fragment in bone matrix enhances osteoclast maturation at a late stage of osteoclast differentiation, J. Bone Miner. Metab 22(5) (2004) 415–429. [PubMed: 15316862]

[15]. Ducy P, Desbois C, Boyce B, Pinero G, Story B, Dunstan C, Smith E, Bonadio J, Goldstein S, Gundberg C, Bradley A, Karsenty G, Increased bone formation in osteocalcin-deficient mice, Nature 382(6590) (1996) 448–52. [PubMed: 8684484]

[16]. Boskey AL, Gadaleta S, Gundberg C, Doty SB, Ducy P, Karsenty G, Fourier transform infrared microspectroscopic analysis of bones of osteocalcin-deficient mice provides insight into the function of osteocalcin, Bone 23(3) (1998) 187–96. [PubMed: 9737340]

[17]. Poundarik AA, Boskey A, Gundberg C, Vashishth D, Biomolecular regulation, composition and nanoarchitecture of bone mineral, Sci. Rep 8(1) (2018) 1191. [PubMed: 29352125]

[18]. Bailey S, Karsenty G, Gundberg C, Vashishth D, Osteocalcin and osteopontin influence bone morphology and mechanical properties, Ann. N.Y. Acad. Sci 1409(1) (2017) 79–84. [PubMed: 29044594]

[19]. Poundarik AA, Diab T, Sroga GE, Ural A, Boskey AL, Gundberg CM, Vashishth D, Dilatational band formation in bone, Proc Natl Acad Sci U S A 109(47) (2012) 19178–83. [PubMed: 23129653]

[20]. Nikel O, Poundarik AA, Bailey S, Vashishth D, Structural role of osteocalcin and osteopontin in energy dissipation in bone, J. Biomech 80 (2018) 45–52. [PubMed: 30205977]

[21]. Gundberg CM, Lian JB, Gallop PM, Measurements of gamma-carboxyglutamate and circulating osteocalcin in normal children and adults, Clin Chim Acta 128(1) (1983) 1–8. [PubMed: 6601547]

[22]. Ingram RT, Park YK, Clarke BL, Fitzpatrick LA, Age- and gender-related changes in the distribution of osteocalcin in the extracellular matrix of normal male and female bone. Possible involvement of osteocalcin in bone remodeling, J. Clin. Invest 93(3) (1994) 989–997. [PubMed: 8132785]

[23]. Okazaki R, Totsuka Y, Hamano K, Ajima M, Miura M, Hirota Y, Hata K, Fukumoto S, Matsumoto T, Metabolic improvement of poorly controlled noninsulin-dependent diabetes mellitus decreases bone turnover, J. Clin. Endocrinol. Metab82(9) (1997) 2915–20. [PubMed: 9284719]

[24]. Heinonen JK, Lahti RJ, A new and convenient colorimetric determination of inorganic orthophosphate and its application to the assay of inorganic pyrophosphatase, Anal. Biochem 113(2) (1981) 313–317. [PubMed: 6116463]

[25]. Hale L, Galvin RS, Risteli J, Ma Y, Harvey A, Yang X, Cain R, Zeng Q, Frolik C, Sato M, PINP: a serum biomarker of bone formation in the rat, Bone 40(4) (2007) 1103–1109. [PubMed: 17258520]

[26]. Garnero P, Ferreras M, Karsdal M, Nicamhlaoibh R, Risteli J, Borel O, Qvist P, Delmas P, Foged N, Delaisse J, The type I collagen fragments ICTP and CTX reveal distinct enzymatic pathways of bone collagen degradation, J. Bone Miner. Res 18(5) (2003) 859–867. [PubMed: 12733725]

[27]. Cole JH, van der Meulen MC, Whole bone mechanics and bone quality, Clin Orthop Relat Res 469(8) (2011) 2139–49.. [PubMed: 21274760]

[28]. Gourion-Arsiquaud S, West PA, Boskey AL, Fourier transform-infrared microspectroscopy and microscopic imaging, Methods Mol Biol 455 (2008) 293–303. [PubMed: 18463826]

[29]. Boskey A, Mendelsohn R, Infrared analysis of bone in health and disease, J Biomed Opt 10(3) (2005) 031102. [PubMed: 16229627]

[30]. Mendelsohn R, Paschalis EP, Boskey AL, Infrared spectroscopy, microscopy, and microscopic imaging of mineralizing tissues: spectra-structure correlations from human iliac crest biopsies, J Biomed Opt 4(1) (1999) 14–21. [PubMed: 23015164]

[31]. Paschalis E, Verdelis K, Doty S, Boskey A, Mendelsohn R, Yamauchi M, Spectroscopic characterization of collagen cross-links in bone, J. Bone Miner. Res 16(10) (2001) 1821–1828. [PubMed: 11585346]

[32]. Spevak L, Flach CR, Hunter T, Mendelsohn R, Boskey A, Fourier transform infrared spectroscopic imaging parameters describing acid phosphate substitution in biologic hydroxyapatite, Calcif. Tiss. Int 92(5) (2013) 418–28.

[33]. Hunter GK, Hauschka PV, Poole AR, Rosenberg LC, Goldberg HA, Nucleation and inhibition of hydroxyapatite formation by mineralized tissue proteins, Biochem. J 317 (Pt 1) (1996) 59–64. [PubMed: 8694787]

[34]. Sugiyama T, Takaki T, Sakanaka K, Sadamaru H, Mori K, Kato Y, Taguchi T, Saito T, Warfarin-induced impairment of cortical bone material quality and compensatory adaptation of cortical bone structure to mechanical stimuli, J. Endocrinol 194(1) (2007) 213–22. [PubMed: 17592035]

[35]. Rey C, Hina A, Tofighi A and Glimcher MJ , Maturation of Poorly Crystalline Apatites: Chemical and Structural Aspects In Vivo and In Vitro, Cells and Mater. 5(4) (1995) 345–356.

[36]. Hunt HB, Donnelly E, Bone Quality Assessment Techniques: Geometric, Compositional, and Mechanical Characterization from Macroscale to Nanoscale, Clin. Rev. Bone Miner. Metab 14(3) (2016) 133–149. [PubMed: 28936129]

[37]. Boskey AL, Bone composition: relationship to bone fragility and antiosteoporotic drug effects, Bonekey Rep 2 (2013) 447. [PubMed: 24501681]

[38]. Yerramshetty JS, Akkus O, The associations between mineral crystallinity and the mechanical properties of human cortical bone, Bone 42(3) (2008) 476–482. [PubMed: 18187375]

[39]. Looker AC, Beck TJ, Orwoll ES, Does body size account for gender differences in femur bone density and geometry?, J. Bone Miner. Res 16(7) (2001) 1291–9. [PubMed: 11450705]

[40]. Callewaert F, Venken K, Kopchick JJ, Torcasio A, van Lenthe GH, Boonen S, Vanderschueren D, Sexual dimorphism in cortical bone size and strength but not density is determined by independent and time-specific actions of sex steroids and IGF-1: evidence from pubertal mouse models, J. Bone Miner. Res 25(3) (2010) 617–26. [PubMed: 19888832]

[41]. Jepsen KJ, Akkus OJ, Majeska RJ, Nadeau JH, Hierarchical relationship between bone traits and mechanical properties in inbred mice, Mamm. Genome 14(2) (2003) 97–104. [PubMed: 12584605]

[42]. Melton LJ 3rd, Epidemiology of hip fractures: implications of the exponential increase with age, Bone 18(3 Suppl) (1996) 121s–125s. [PubMed: 8777076]

[43]. Yates LB, Karasik D, Beck TJ, Cupples LA, Kiel DP, Hip structural geometry in old and old-old age: similarities and differences between men and women, Bone 41(4) (2007) 722–32. [PubMed: 17662680]

[44]. de L II, van der Klift M, de Laet CE, van Daele PL, Hofman A, Pols HA, Bone mineral density and fracture risk in type-2 diabetes mellitus: the Rotterdam Study, Osteoporos Int 16(12) (2005) 1713–20. [PubMed: 15940395]

[45]. Schwartz AV, Vittinghoff E, Bauer DC, Hillier TA, Strotmeyer ES, Ensrud KE, Donaldson MG, Cauley JA, Harris TB, Koster A, Womack CR, Palermo L, Black DM, Association of BMD and FRAX score with risk of fracture in older adults with type 2 diabetes, Jama 305(21) (2011) 2184–92. [PubMed: 21632482]

Highlights

1. Female 6 month old Osteocalcin knock-out mice (OC−/−) on a C57BL/6J background had increased bone formation, and no change in resorption as compared to C57BL/6J (OC+/+).
2. OC−/− bones had a more immature mineral phase, increased carbonate in mineral and decreased crystallinity as compared to OC+/+ bones.
3. A lower bone mineral density and lower mineral/matrix ratio observed in OC −/− cortical bones as compared to OC+/+ bones.
4. Weaker bone material qualities resulted in reduced stiffness and strength in OC−/− as compared to OC+/+ bone.
5. In contrast, OC−/− mice on mixed background (129/B6) had increased cortical thickness, increased bone mineral density and increased bone strength. Some mineral parameters are dependent on genetic background in OC−/− mice.

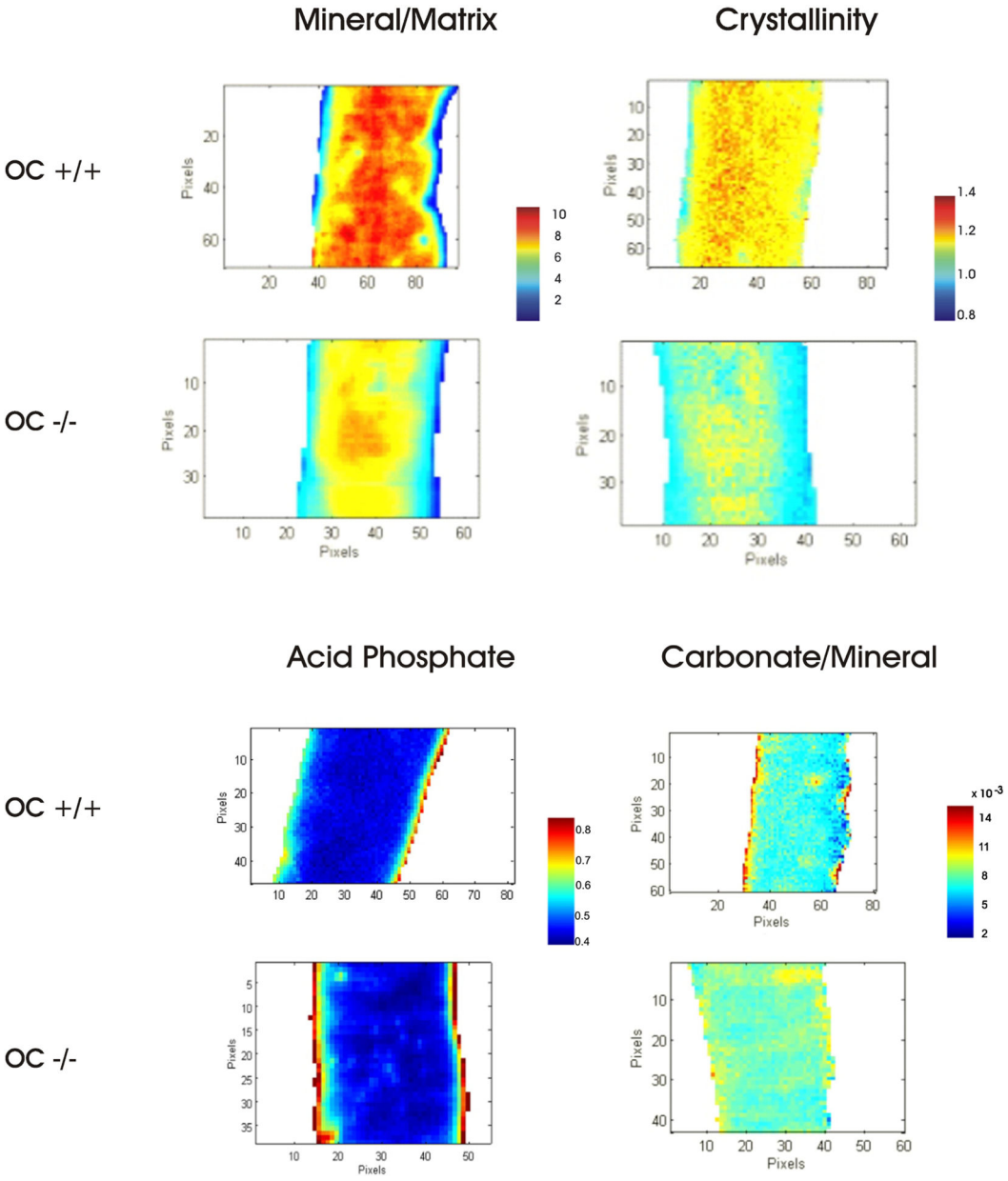

Figure 1:

Cortical bone FTIR images of mineral/matrix ratio, crystallinity, acid phosphate (HPO_4^{2-}) substitution in cortical mineral and carbonate to mineral ratios for OC+/+ and OC−/− bones.

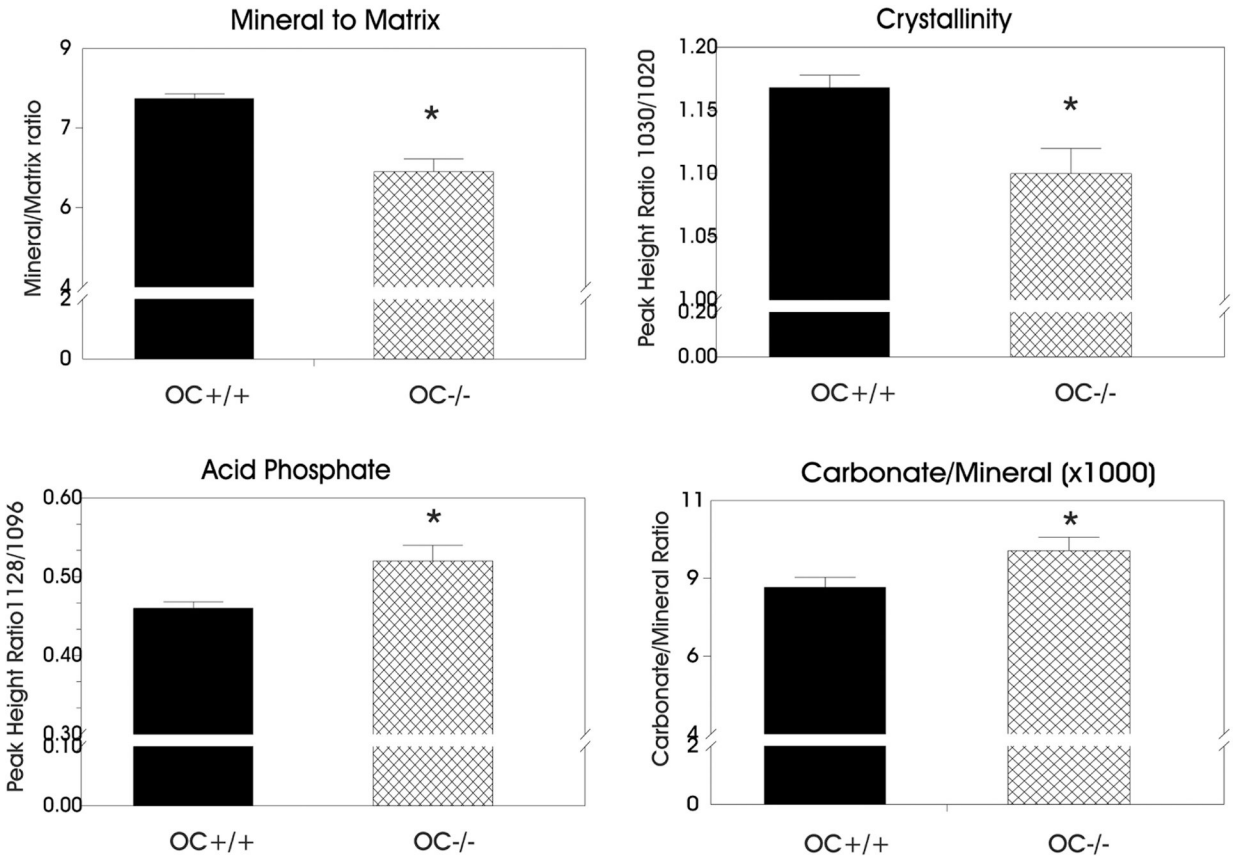

Figure 2:

Plots of FTIR imaging parameters for cortical bone. Asterisks indicate significant differences compared to WT OC+/+ (* $p<0.05$, see text).

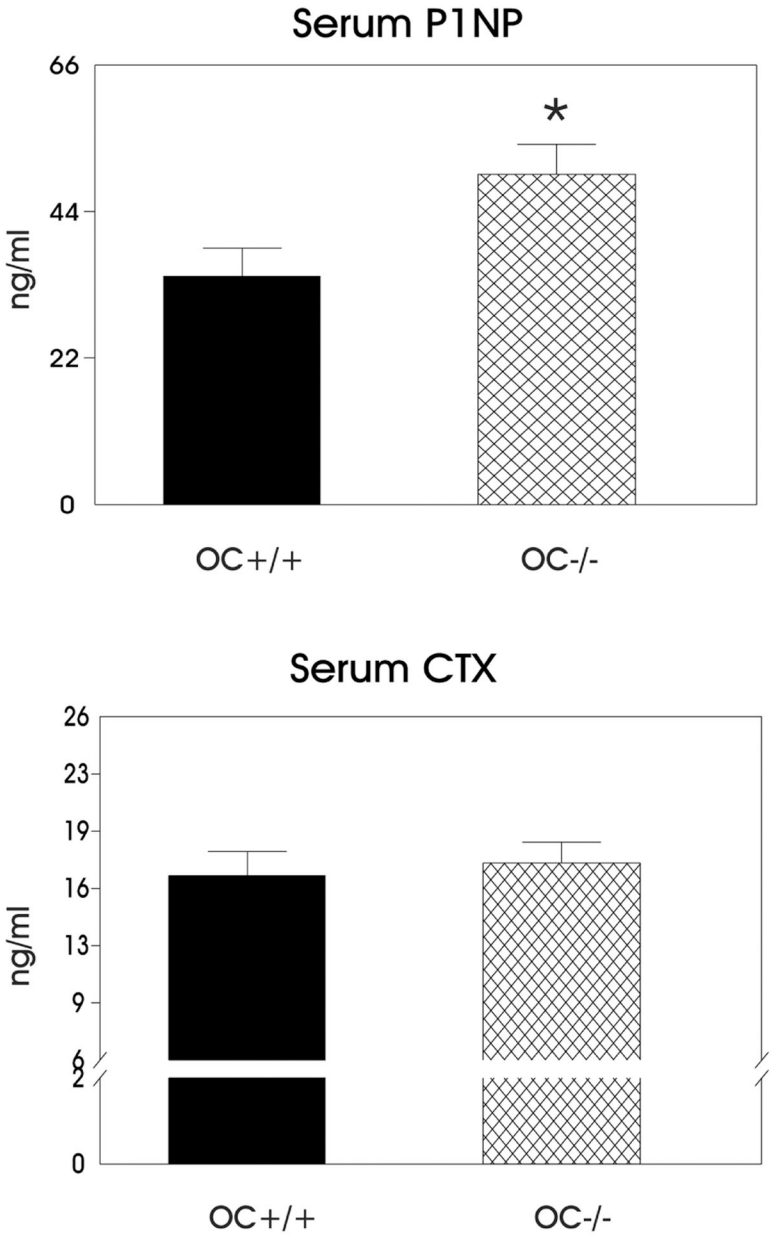

Figure 3:
Plots of serum biomarkers P1NP (bone formation) and CTX (bone resorption). The asterisk indicates a significant difference as compared to the WT OC+/+ bones ($p < 0.05$).

Table IA:

MicroCt Parameters for Cortical Bone

	CORTICAL BONE		
Parameter	**OC+/+**	**OC−/−**	**p value**
TV (mm^3)	0.77 +/− 0.01	0.77 +/− 0.01	n.s.
BV (mm^3)	0.33 +/− 0.01	0.34 +/− 0.01	n.s.
BV/TV	0.44 +/− 0.01	0.44 +/− 0.01	n.s.
TMD (mg/cm^3)	1089.2 +/− 4.48	1069.5 +/− 5.9	p<0.01
Ct. Th. (mm)	0.188 +/− 0.003	0.188 +/− 0.003	n.s
Bone Area (mm^2)	0.77 +/− 0.01	0.78 +/− 0.01	n.s
Marrow Area (mm^2)	0.99 +/− 0.02	0.98 +/− 0.01	n.s
Total Area (mm^2)	1.76 +/− 0.03	1.76 +/− 0.02	n.s
I_{min} (mm^4)	0.111 +/− 0.004	0.109 +/− 0.003	n.s
I_{max} (mm^4)	0.226 +/− 0.008	0.234 +/− 0.007	n.s
J (mm^4)	0.34 +/− 0.01	0.34 +/− 0.01	n.s
Sample size (N)	11	10	

Bone voume to total volume (BV/TV), cortical thickness (Ct. Th.) tissue mineral density TMD.

Table IB:

MicroCT Parameters for Trabecular Bone

Trabecular Bone			
Parameter	**OC+/+**	**OC−/−**	**P value**
TV (mm^3)	1.42 +/− 0.03	1.41 +/− 0.02	n.s.
BV (mm^3)	0.13 +/− 0.007	0.18 +/− 0.01	$p < 0.001$
BV/TV (%)	9.1 +/− 0.6	12.4 +/− 0.7	$p < 0.001$
Conn-Dens, (mm^{-1})	11.5 +/− 2.0	25.2 +/− 1.0	$p < 0.001$
Tb.N.	1.90 +/− 0.06	2.18 +/− 0.06	$p < 0.001$
Tb. Th.	0.07 +/− 0.001	0.07 +/− 0.002	n.s.
Tb. Sp.	0.52 +/− 0.01	0.46 +/− 0.01	$p < 0.001$
TMD (mm^{-3})	874.7 +/− 4.6	869.4 +/− 9.8	n.s.
Sample Size (N)	10	10	

Connectivity density (Conn-Dens), trabecular number (Tb. N.), trabecular thickness (Tb. Th.) and trabecular spacing (Tb. Sp.).

Table II.

Mechanical properties of femurs tested in three-point bending. Asterisk(s) indicate significant difference compared to WT OC+/+ (*p<0.05, **p<0.01) and an exclamation point (!) indicates a trend (p=0.056).

Parameter	**OC+/+**	**OC−/−**
Bending Stiffness (El) N-mm^2	920 +/− 54	765+/− 45*
Size-adjusted bending stiffness (EI/I_{min}) N/mm^2	8340 +/− 503	7014 +/− 401!
Maximum Bending Moment (M_{max}) N-mm	37.0+/−1.0	32.6 +/− 0.9**
Size-Adjusted Maximum Bending Moment (M_{max}/I_{min}) N/mm^3	337 +/− 14	299 +/− 9.0*
Sample size (N)	11	10

Table III.

Histomorphometric measurements of the number of osteoclasts and osteoblasts on the endocortical bone of OC+/+ and OC−/− mice. Asterisk indicates a significant difference compared to OC+/+ (*p<0.01).

Measurement	**OC+/+**	**OC−/−**
No. osteoblasts/bone perimeter	31.8 +/− 0.6	45.7 +/− 3.4*
No. of osteoclasts/bone perimeter	0.39 +/− 0.02	0.37 +/− 0.09
Sample size (N)	4	5